DELPHI 97-90 CONF 76
28 July, 1997

Search for charginos mass-degenerate with the LSP

Preliminary

DELPHI Collaboration

C. Lacasta[a], **F.L. Navarria**[b], **S. Navas**[a], **S. Paiano**[b], **A. Perrotta**[b], **P. Rebecchi**[c], **T. Rovelli**[b], **M.G. Verardi**[b]

[a] IFIC, Valencia-CSIC, and D.F.A.M.N., U. de Valencia, Avda. Dr. Moliner 50, E-46100 Burjassot (Valencia), Spain

[b] Dipartimento di Fisica, Università di Bologna and INFN, via B. Pichat 6/2, I-40127 Bologna, Italy

[c] CERN, CH-1211 Geneva 23, Switzerland

Abstract

The search for SUSY particles almost mass-degenerate with the Lightest Supersymmetric Particle requires different strategies with respect to the usual search methods. If R-parity is conserved, the visible products at the end of the SUSY decay chain are usually very soft, and therefore difficult both to detect and to separate from the standard backgrounds. As an attempt to cope with these difficulties, a search for charginos mass-degenerate with the lightest neutralino has been performed in DELPHI using a photon radiated from the initial state as a tag. In extremely degenerate scenarios the lifetime of the SUSY particle generated at the interaction point can be large enough to produce either visible secondary vertices or decays outside the detector: evidence for quasi-stable heavy charged particles or for displaced decay vertices has been searched for.

Paper submitted to the LP'97 Conference
Hamburg, July 28 - August 1st

1 Introduction

Supersymmetry (SUSY) [1] is one of the most appealing theories since it is able to extend the validity of the Standard Model (SM) towards the high energy domain near the Planck scale. Its simplest representation is the so called Minimal Supersymmetric Standard Model (MSSM), in which the particle and field content is kept as low as possible: all ordinary particles have their corresponding supersymmetric partner (sparticle). Only the number of (complex) higgs doublets must be enlarged with respect to the SM, to avoid anomalies in the theory: in the MSSM they are set to two.

The well tested lepton and baryon number conservation favours supersymmetric theories in which the R-parity is conserved. It follows that sparticles cannot decay into ordinary particles alone; instead, there must exist a lightest supersymmetric particle (LSP) which is stable and remains as an ash of any SUSY decay chain. The non observation of exotic nuclei with strange charge-to-mass ratio [2] suggests that an heavy LSP can only be neutral and weakly interacting. Thus, the final result of an e^+e^- annihilation into a pair of sparticles consists always in visible ordinary particles plus the missing energy carried away by the (at least) two LSP's. The normal way of probing SUSY is therefore to look for particles accompanied by some missing energy. This works as far as the mass difference between the produced sparticle and the LSP is large enough to leave some sizeable amount of energy for the final state particles. Typically, the searches carried out so far at LEP in the different SUSY channels reach mass differences of a few GeV/c^2. DELPHI at LEP2 gives exclusion limits for charginos, neutralinos, sleptons and $\tilde{b}$ and $\tilde{t}$ squarks, provided that the mass difference between the sparticles searched for and the LSP is above 3 to 5 GeV/c^2 [3, 4]. For smaller mass differences, the only limits available so far are those obtained at LEP1, which ruled out charged SUSY particles lighter than about $M_Z/2$ [5].

The SUSY particles do not have the same mass as their ordinary matter superpartners. This means that supersymmmetry is not an exact symmetry, but it must be broken at low energies. Different models are characterized by how the SUSY breaking is inserted into the theory. One can assume that SUSY is embedded into an underlying theory in which the supersymmetry is broken thanks to the non-zero vacuum expectation values assumed by some auxiliary fields. Four-dimensional strings have natural candidates: the dilaton and the moduli superfields [6]. In particular, if the SUSY breaking is dominated by the overall 'size' modulus field, a scenario in which the lightest chargino and neutralino are closely mass-degenerate is quite likely [7]. Also in other models degeneracy between the lightest chargino and neutralino can take place, although this appears to be in a corner of the space of the SUSY parameters. It is important to have some experimental sensitivity also for these scenarios in which there is degeneracy between the lowest lying SUSY particles.

What are the technical challenges of the low ΔM region? Let us consider the case of the chargino. If $\Delta M \equiv M_{\tilde{\chi}_1^\pm} - M_{\tilde{\chi}_1^0}$ is very low, the chargino lifetime can be so long that it passes through the whole detector without decaying. In DELPHI such a possibility is covered by looking for heavy charged particles identified with the RICHes and/or releasing an anomalously high ionization in the TPC [8]. The region with ΔM of a few hundred MeV/c^2 can be covered by looking for visible kinks or reconstructed secondary vertices originating from a chargino decay inside the detector but significantly displaced from the main interaction point [9].

For larger ΔM the chargino decay length is so short that the decay vertex cannot be distingushed from the production one. However, the visible particles carry only a small fraction of the initial energy. Usual cuts against $\gamma\gamma$ events require a minimum visible tranverse momentum (P_T), and result in large inefficiencies, if not in complete blindness to chargino decays. On the other hand, it is not possible to remove the P_T cut completely without being flooded with the $\gamma\gamma$ background, which has a cross section orders of magnitude higher than any signal searched for at LEP2. Here a suggestion initially proposed in [10] is applied to search for these events. If one considers the events accompanied by a hard photon radiated in the initial state (ISR), then the $\gamma\gamma$ background can be kept under control by choosing the photon transverse energy to be greater than

$$(E_\gamma^T)^{min} = \sqrt{s} \cdot \frac{\sin\theta_{min}}{1+\sin\theta_{min}} \quad . \tag{1}$$

θ_{min} is the lowest polar angle accessible in the detector, defined by the inner acceptance of the DELPHI luminometer. Therefore one of the final state electrons, which usually escapes undetected in the beam pipe in a $\gamma\gamma$ event, should be deflected at an angle larger than θ_{min}, and allows for identification of the event as a background one. The price to be paid with such a selection is in terms of the efficiency: only a few percent of the SUSY events has an ISR photon with $E_\gamma^T > (E_\gamma^T)^{min}$, given the θ_{min}. On the other hand, the highly energetic photon can help in triggering the event and recover to the inefficiency due to the softness of the visible decay products of the chargino.

Only mass-degenerate charginos and neutralinos are considered in this paper. The selection [8] and an *ad hoc* modification of [9] is applied here to look for charginos extremely mass-degenerate with the neutralino. The analysis which uses the ISR tag to cover the interval of degeneracy between 0.5 and 3 GeV/c^2 is discussed next. At the upper end of this interval, this analysis is combined with the 'traditional' search for charginos in DELPHI [4], to improve the lower limit on the chargino mass.

2 Data samples and event generators

A detailed description of the DELPHI detector and its performances can be found in [11]. During the high energy runs of LEP in 1995-96, DELPHI collected data at the centre-of-mass energies of 130, 136, 161 and 172 GeV. Only those runs in which the relevant subdetectors worked correctly were taken into account for each analysis. The luminosities used at the different energies were approximately 3, 3, 10 and 10 pb^{-1}.

To evaluate the signal efficiency and the background contamination, events were generated using several different programs, all relying on JETSET 7.4 [12] for quark fragmentation. All the events generated were passed through a complete simulation of the DELPHI detector [13], and then processed in exactly the same way as the real data.

The program SUSYGEN [14], which includes ISR, was used to simulate all supersymmetric events. Version 1 was used in the search with the ISR photon tag (section 5); version 2 was used in the search for visible decay lenghts (section 4). The version 2 of this generator includes the final state radiation. The formula used to compute the leptonic decay widths (i.e. branching ratios and lifetimes) has been modified since version 1 in order to reproduce the results of the analytical calculation reported in [7] for the very degenerate cases in which the hadronic chargino decays are almost negligible.

For the SM background, several samples of the different final states were generated with statistics which were at least 3-4 times those expected. Radiative Z^0 decays ($e^+e^- \to Z^0\gamma$, $Z^0 \to$ anything) and four-fermion processes were generated with PYTHIA [12]. For the $\gamma\gamma$ collisions, the generator of Berends, Daverveldt and Kleiss (BDK) [15] was used for the leptonic final states. In this generator the $(e^+e^-)\mu^+\mu^-$ and $(e^+e^-)\tau^+\tau^-$ events include the simulation of the transverse energy of the ISR photon, while in $(e^+e^-)e^+e^-$ events it is not implemented. In the $\gamma\gamma$ collisions leading to hadronic final states, the QCD and VDM parts were simulated with the TWOGAM [16] generator in which no transverse energy is associated to the ISR photon. BDK, with visible ISR, was used for the QPM part. Although not used for the computation of the background, $\gamma\gamma \to$ QPM events were also generated using the TWOGAM generator, to study the differences between the two codes, mainly those related to the absence of ISR photons with visible transverse energy in TWOGAM.

3 Chargino and neutralino production and decay at low $\Delta(M)$

The Higgsino and gaugino sector of the MSSM can be described in term of four parameters: the ratio $\tan\beta$ of the two Higgs vacuum expectation values, the Higgs mixing parameter μ, the $SU(2)$ gaugino mass M_2 and the $U(1)$ gaugino mass M_1. In most models the gaugino mass unification is assumed at the GUT scale, which gives a relation between M_1 and M_2

$$M_1 = \frac{5}{3}\tan^2\theta_W \cdot M_2 \simeq 0.5 \cdot M_2 \quad . \tag{2}$$

However, the unification condition above is not strictly necessary in the theory and several models exist without it: in particular, the SUSY-string scenario proposed in [7]. The definition

$$M_1 = R_f \cdot \frac{5}{3}\tan^2\theta_W \cdot M_2 \quad , \tag{3}$$

will be used, so that any value of R_f different from 1 indicates how much the model deviates from the gaugino mass unification hypothesis.

In the MSSM there are two charginos ($\tilde{\chi}_1^\pm$ and $\tilde{\chi}_2^\pm$). These mass eigenstates are linear combinations of the two interaction eigenstates, the wino and the charged higgsino. Also four neutralinos exist, linear combinations of the neutral interaction eigenstates. In the following it will be assumed that the lightest neutralino is the LSP.

The lightest chargino is mass-degenerate with the LSP in two cases [7]:

- Low μ, large $M_{1,2}$ scenario: $\tilde{\chi}_1^0$ and $\tilde{\chi}_1^+$ are both higgsino-like and nearly degenerate, with masses $\sim \mu$;
- High μ, low M_2: the $\tilde{\chi}_1^0$ and the $\tilde{\chi}_1^+$ are both gaugino-like and degenerate with masses $\sim M_2$. In this scenario, in order to have ΔM of the order of 1 GeV/c^2 or smaller, R_f from eq. (3) must be larger than or equal to 2.

In the first scenario, the next-to-lightest neutralino is also mass-degenerate with the lightest neutralino, with a mass splitting which is approximately twice the chargino one. The same is true also for the second scenario, but only for $R_f \simeq 2$.

3.1 Cross sections

The $e^+e^- \to \tilde{\chi}_1^+\tilde{\chi}_1^-$ and $e^+e^- \to \tilde{\chi}_1^0\tilde{\chi}_2^0$ cross sections [14] at the four centre-of-mass energies are shown in figures 1 and 2, as a function of the $\tilde{\chi}_1^\pm$ and $\tilde{\chi}_2^0$ mass. R_f is set to 1 in the higgsino case (lower bands in the figures) and to 2 in the gaugino case (upper bands, not visible in the plots of the neutralino cross section). In the first case the cross sections

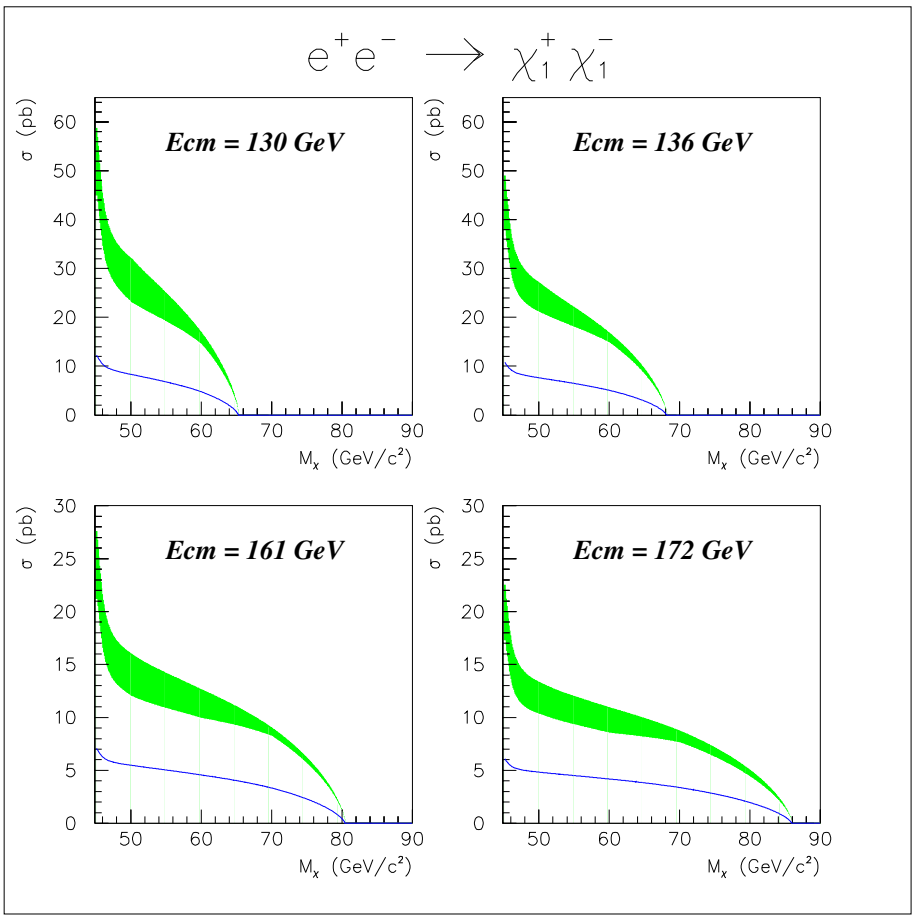

Figure 1: $e^+e^- \to \tilde{\chi}_1^+\tilde{\chi}_1^-$ *cross sections as a function of the chargino mass at four centre-of-mass energies. The upper bands refer to the* $M_2 \ll |\mu|$ *gaugino-like scenario; the lower bands to the* $|\mu| \ll M_2$ *higgsino-like one. The width of the two bands allows for a variation of the parameters within the intervals:* $0.5 < \Delta M < 3$ *GeV/*c^2*;* $1 < \tan\beta < 50$*;* $M_{\tilde{\nu}} > 500$ *GeV/*c^2 *(gaugino) or* $M_{\tilde{\nu}} > M_{\tilde{\chi}_1^+}$ *(higgsino).*

are stable when varying R_f from 1 to 10, and also in the second case the cross sections do not change by more than 5-6% if R_f moves between 2 and 10. The non-zero widths of the bands arise from a variation of $\tan\beta$ from 1 to 50 and from a variation of M_2 and μ over all values that are compatible with the chargino mass and mass differences between 0.5 and 3 GeV/c^2 (lower mass differences do not alter the behaviour of the cross sections). The exchange of sfermions in the t-channel interferes destructively with the s-channel production, lowering the gaugino cross section at small values of $M_{\tilde{\nu}}$ for chargino production and of $M_{\tilde{e}}$ for the neutralino case. In the figures, the slepton mass has been varied from $M_{\tilde{\chi}}$ to 1 TeV/c^2 in the higgsino plots, and from 500 GeV/c^2 to 1 TeV/c^2 in the gaugino ones.

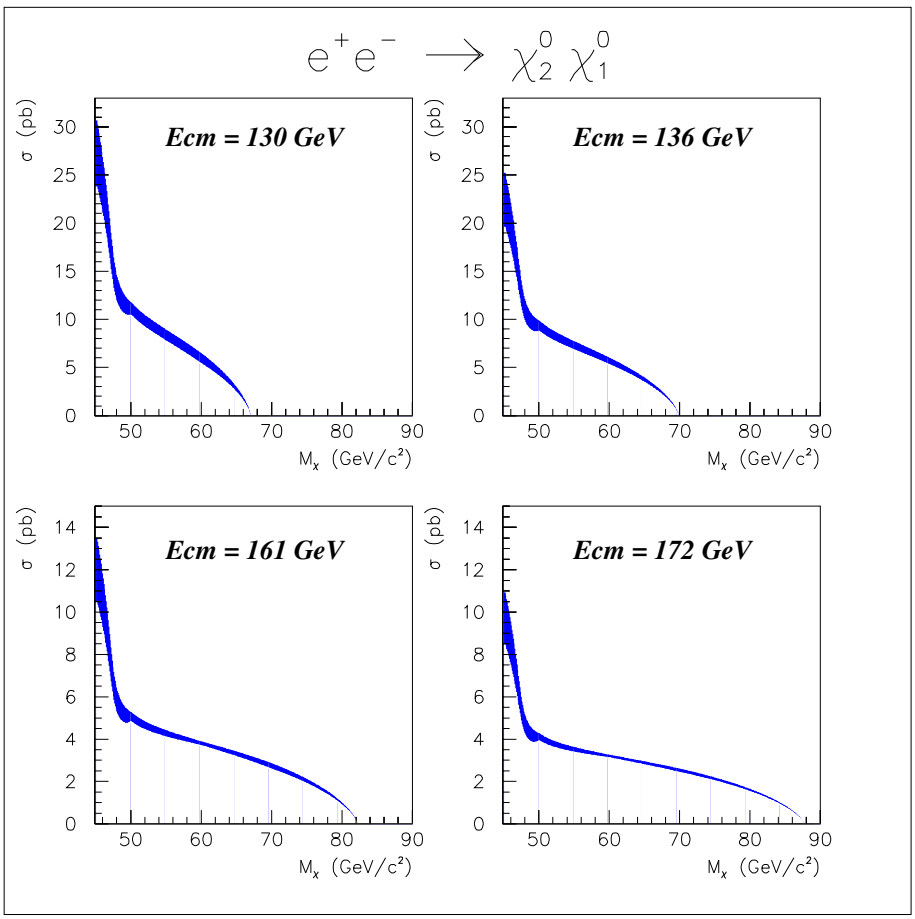

Figure 2: $e^+e^- \to \tilde{\chi}_1^0\tilde{\chi}_2^0$ *cross sections as a function of the* $\tilde{\chi}_2^0$ *mass at four centre-of-mass energies. Only the higgsino-like scenario* ($|\mu| \ll M_2$) *is shown, because the cross sections are of the order of one fb in the gaugino case. The width of the bands allows for a variation of the parameters within the intervals:* $0.5 < \Delta M < 3$ *GeV*$/c^2$; $1 < \tan\beta < 50$; $1 < R_f < 10$; $M_{\tilde{e}} > M_{\tilde{\chi}_2^0}$.

For the neutralinos, the $e^+e^- \to \tilde{\chi}_1^0\tilde{\chi}_1^0$ and $e^+e^- \to \tilde{\chi}_2^0\tilde{\chi}_2^0$ cross sections are much smaller than the $e^+e^- \to \tilde{\chi}_1^0\tilde{\chi}_2^0$ one, shown in fig. 2. This last process is the only one considered in the following for the production of neutralinos.

The chargino cross sections is approximately three times larger in the gaugino-like scenario than in the higgsino-like one. On the contrary, the $e^+e^- \to \tilde{\chi}_1^0\tilde{\chi}_2^0$ cross section in the gaugino-like scenario is more than three orders of magnitude smaller than in the higgsino one.

3.2 Branching ratios and lifetimes

Since the number of signal events potentially visible in the data depends both on the cross section and on the efficiency of the selection criteria, the *inos* lifetimes and decay modes are quite important for the analysis.

The partial decay widths of the chargino in SUSYGEN 2 have been compared with the analytical calculation of [7]. The latter takes only into account the chargino decay through W exchange, thus for the comparison $m_{\tilde{\nu}}$ has been set extremely heavy, 1 TeV$/c^2$,

in SUSYGEN 2. The comparison of the Branching Ratios (BR) computed in the two cases is shown in figure 3a, for a chargino of 50 GeV/c^2 and degeneracies between 100 MeV/c^2 and 5 GeV/c^2. The analytical calculation uses the form factors of the hadronic resonances to determine the shape of the hadronic width for $\Delta M < 2$ GeV/c^2. This treatment describes correctly the τ decays, i.e. decays with $\Delta M = m_\tau$ [7]. SUSYGEN instead generates a pair of quarks and hadronizes them afterwords. This explains the difference in the hadronic widths (see fig. 3a). However, the leptonic widths agree nicely in the two programs.

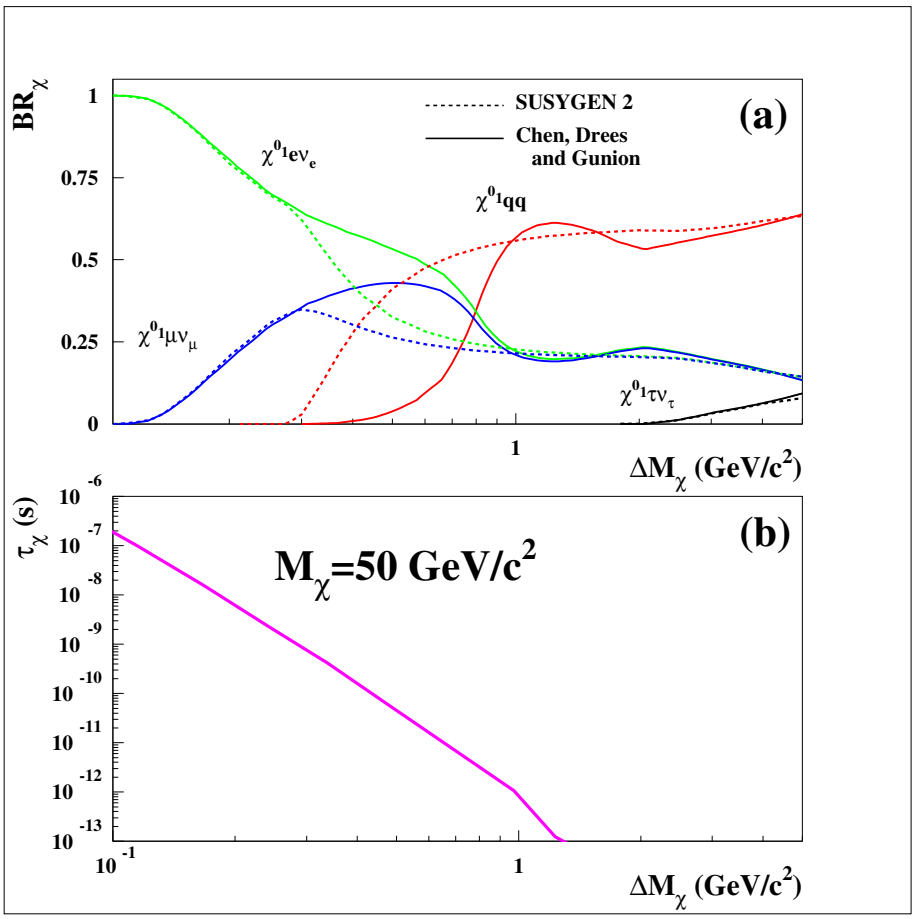

Figure 3: *Branching ratios (a) and lifetime (b) of a 50 GeV/c^2 chargino decaying into the LSP plus standard particles, as a function of the mass difference between the chargino and the LSP. The sneutrino mass has been set to 1 TeV/c^2, to avoid the $\tilde{\nu}$ contribution. The branching ratios of SUSYGEN 2 (dashed line) and the analytical calculation [7] (full line) are compared as a function of ΔM.*

Figure 3b shows the lifetime of a 50 GeV/c^2 gaugino-like chargino as a function of ΔM, in the case of heavy sneutrinos. A relevant feature of the chargino decays at low ΔM is that lifetime and BR's depend very little on the scenario choosen: as far as the decays through scalar exchange can be neglected, they only depend on ΔM.

Figure 4 shows the exclusive branching ratios for the second neutralino as a function of ΔM, in the two scenarios which allow for degenerate state. Unlike the chargino case, there is now a strong model dependence of the decay width. In the higgsino scenario, the only one with a non negligible cross-section, the rate of the radiative decay $\tilde{\chi}^0_2 \to \tilde{\chi}^0_1 \gamma$

increases together with the degeneracy. In the region of interest for the present study, a relevant fraction of the $\tilde{\chi}_2^0$ ends up in a photon or in a pair of neutrinos, besides the LSP. It is hard to unambiguously detect a photon of less than 1 GeV in the detector and separate it from the background; thus, in the higgsino scenario a relevant fraction of the $\tilde{\chi}_2^0$, when degenerate with the $\tilde{\chi}_1^0$, ends up in an absolutely or practically invisible final state. This is the reason why in both scenarios the present work has been limited to the search for degenerate charginos, leaving neutralinos aside.

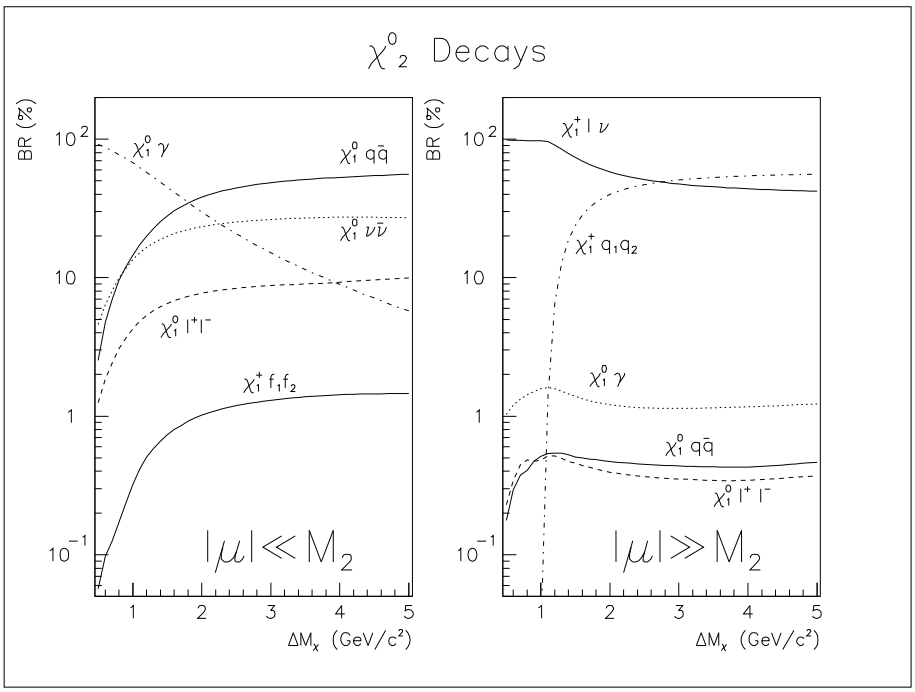

Figure 4: *Branching ratios of the decay modes of the second neutralino, when the mass difference between the $\tilde{\chi}_2^0$ and the LSP is below 5 GeV/c^2. The left (right) plot refers to the higgsino-like (gaugino-like) scenario.*

4 Search for charginos with a visible decay length

At present, three methods are used in DELPHI to look for heavy particles with a visible decay length. The reader interested in the details of the individual analyses should refer to the papers describing the searches for sleptons, [8], [9].

4.1 Heavy, 'stable' charged particles

Heavy, stable or almost stable charged particles are identified through their anomalously high specific ionization in the TPC or by the absence of Cherenkov light produced in the two radiators of the barrel RICH [8]. Figure 4(a) in [8] shows the efficiency for pair produced heavy particles as a function of their mass and of the centre-of-mass energy, in the hypothesis that both particles cross the whole detector. Results on the search for stable charginos, i.e. for ΔM less than about 100 MeV/c^2, have already been published by DELPHI [8]. In case of larger ΔM, the detection efficiency can be obtained by convoluting

the stable particles efficiency with the probability that the particle decays outside the relevant parts of the detector.

The trigger efficiency for heavy tracks crossing the whole TPC and the RICH is one.

4.2 Kinks

If the heavy particle decays inside the central tracking devices of DELPHI (at a radius comprised between 10 cm and 1 m), then both the mother and the daughter track can be reconstructed, forming an angle between their directions. A search in DELPHI for staus decaying into a light gravitino and an ordinary tau lepton uses this method [9]. In the search for long-lived mass-degenerate charginos, the efficiency for a single vertex reconstruction, as a function of the radial distance to the beam spot, cannot be taken directly from [9]. In the present case the visible momentum of the decay products is quite small (typically less than 1 GeV/c), thus rendering more difficult the identification of the secondary track and, therefore, of the kink. In the analysis for the degenerate charginos, the minimum momentum allowed for the charged tracks has been lowered from 500 to 100 MeV/c. To reduce the background, mainly coming from beam-gas collisions, the typical topology of the degenerate chargino events is exploited: two particles emitted in opposite emispheres with, at most, one visible, although soft, charged daughter each. In particular, with respect to the search for long lived $\tilde{\tau}$ the overall maximum track multiplicity has been reduced from 10 to 5 and the minimum momentum allowed for the daughter track from 1.5 GeV/c to 100 MeV/c. The background is kept under control by dividing the event in two emispheres, defined by the direction of the line connecting the main vertex to the kink. Then, at least one track (and less than three) must be found in each emisphere: beam gas events tend to be fully contained into a single emisphere.

This selection was applied to samples of degenerate charginos, generated at $\sqrt{s} = 161$ and 172 GeV and passed through the full DELPHI simulation and reconstruction chain. In particular, chargino masses of 40, 50, 60, 70, 75 GeV/c^2 and degeneracies, respectively, of 270, 270, 260, 230, 210 MeV/c^2 were generated at 161 GeV. Analogously, at 172 GeV the masses and degeneracies generated were respectively 40, 50, 60, 70, 80 GeV/c^2 and 290, 290, 270 , 250, 200 MeV/c^2. The efficencies for the single vertex reconstruction as a function of the radial distance of the decay to the beam spot are plotted in figure 5. The efficiencies for the 60 GeV/c^2 sample and those for the sample with the heaviest mass are shown at both energies. The efficiencies are practically flat between 20 and 90 cm for almost all the masses generated and tend to decrease only when approaching the kinematical limit. This happens because the reduced boost cannot result in a sufficiently large momentum of the secondaries. The dependence of the selection efficiency on ΔM is low: it tends to grow together with ΔM, as the mean momentum of the decay products increases.

The efficiency for triggering and preselecting these events (ε_{trigg}) depends on the mass of the chargino and on the centre-of-mass energy (table 1). The total efficiency for a pair of degenerate charginos, each creating a kink inside DELPHI at radii r_1 and r_2 can then be obtained as

$$\varepsilon_{tot} = \varepsilon_{trigg} \cdot [\varepsilon_{vtx}(r_1) + (1 - \varepsilon_{vtx}(r_1)) \cdot \varepsilon_{vtx}(r_2)] \tag{4}$$

where $\varepsilon_{vtx}(r)$ is the single kink reconstruction efficiency.

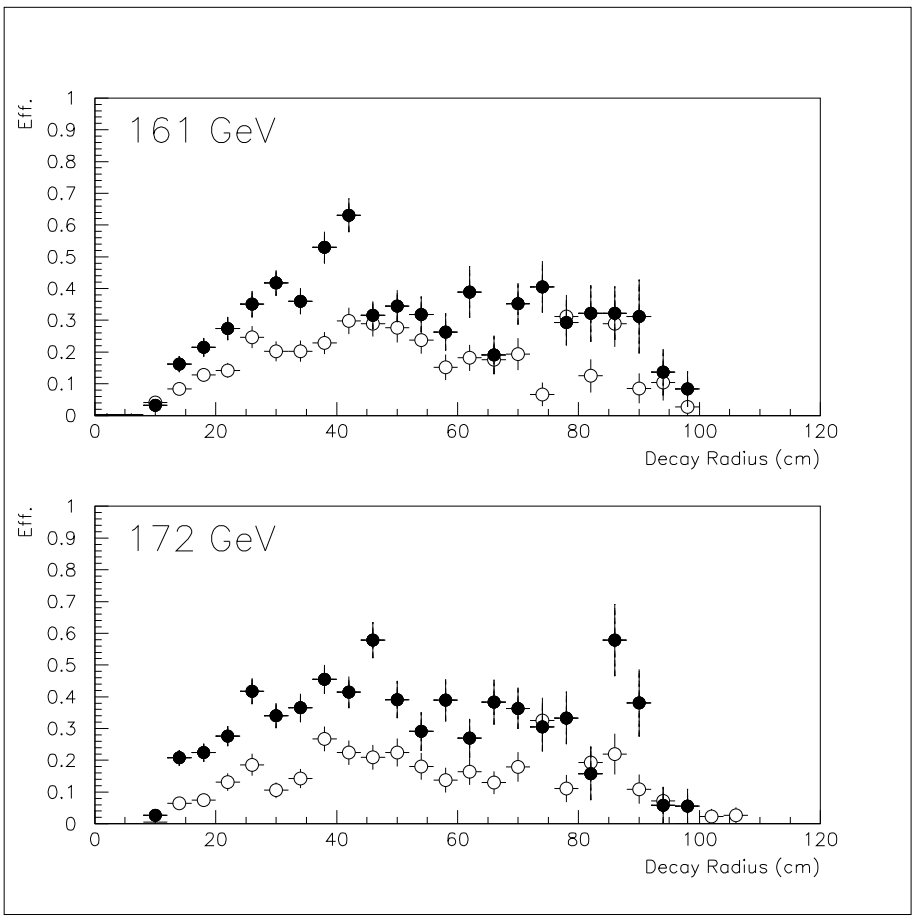

Figure 5: *Efficiency for the kink reconstruction as a function of the chargino decay radius, at the centre-of-mass energies of* 161 *and* 172 *GeV. Black dots refer to chargino masses of* 60 GeV/c^2 *and* $\Delta M = 260$ *and* 270 MeV/c^2*, respectively; white dots refer to chargino masses of* 75 *and* 80 GeV/c^2 *and degeneracies of* 210 *and* 200 MeV/c^2*, respectively.*

4.3 Global efficiency for charginos with visible decay length

The selections in the search for long lived charginos yield an efficiency which is a function of the decay radius of the chargino. Each chargino in DELPHI can be tagged by one of the two searches: if it decays outside the RICH, by the search for stable charged particles; if it decays between the beginning of the ID and the end of the TPC, by the search for kinks. The search for displaced vertices, when the chargino decays before the VD, has not yet been finalised. The global DELPHI efficiency, which is a function of the decay radius, is given by the logical OR of the selection criteria.

The chargino decay length follows an exponential law, and the probability that the decay happens at a radius x is

$$\frac{1}{\lambda_{\tilde{\chi}}} \cdot \exp\left(-\frac{x}{\lambda_{\tilde{\chi}}}\right) \quad , \tag{5}$$

where $\lambda_{\tilde{\chi}}$ is the mean decay length which, in the laboratory frame, depends on the

	$E_{cms} = 161$ GeV				
$M_{\tilde{\chi}}$ (GeV/c^2)	40	50	60	70	75
ΔM (MeV/c^2)	270	270	260	230	210
ε_{trigg}	81.1%	89.5%	85.7%	85.3%	81.2%
	$E_{cms} = 172$ GeV				
$M_{\tilde{\chi}}$ (GeV/c^2)	40	50	60	70	80
ΔM (MeV/c^2)	290	290	270	250	200
ε_{trigg}	90.4%	94.7%	86.3%	87.8%	82.2%

Table 1: *Trigger efficiency in the search for kinks, computed on the samples of degenerate charginos used in the analysis.*

(squared) available centre-of-mass energy s' through:

$$\lambda_{\tilde{\chi}} = \sqrt{\frac{s'}{4M_{\tilde{\chi}}^2} - 1} \cdot \tau_{\tilde{\chi}} \cdot c \quad . \tag{6}$$

The lifetime is mainly determined by ΔM and $M_{\tilde{\nu}}$. However the dependence on $M_{\tilde{\chi}}$ is taken into account as well.

$\lambda_{\tilde{\chi}}$ depends on the available centre-of-mass energy, after a possible radiation of a photon from the initial state, $s' = sz$. Then

$$p(x) = \int_0^1 dz \left[\frac{1}{\sqrt{\frac{sz}{4M_{\tilde{\chi}}^2} - 1} \cdot \tau_{\tilde{\chi}} \cdot c} \cdot \exp\left(- \frac{x}{\sqrt{\frac{sz}{4M_{\tilde{\chi}}^2} - 1} \cdot \tau_{\tilde{\chi}} \cdot c} \right) \cdot G(z) \right] \tag{7}$$

where $G(z)$ is the radiation function, which depends on the behaviour of the chargino cross section.

Since the probability that the chargino decays at x and passes the (single arm) selection criteria is $p(x)\varepsilon(x)$, the overall probability that the chargino decays between two radii a and b and is selected is:

$$P(a, b, M_{\tilde{\chi}}, \Delta M) = \int_a^b p(x)\varepsilon(x)\, dx \quad . \tag{8}$$

Using the selection efficiencies as step functions (as for example in figure 5), one of the two integrals can be solved analytically, and one has:

$$P(a, b, M_{\tilde{\chi}}, \Delta M) = \int_0^1 dz\, G(z) \sum_{x_i \in (a,b)} \varepsilon_i \left(e^{-\frac{x_i}{\lambda_{\tilde{\chi}}(zs)}} - e^{-\frac{x_i+1}{\lambda_{\tilde{\chi}}(zs)}} \right) \tag{9}$$

The formula above gives the probability to select a single chargino of mass $M_{\tilde{\chi}}$ and degeneracy ΔM at a given $\sqrt{s}$. The event selection probability is then given by the logical

OR of the two single particles probabilities, multiplied by the overall trigger efficiency as in eq. (4).

The effect of the reduction of the decay length by an ISR photon is not always negligible. Figure 6a shows the mean decay length $\lambda_0(\sqrt{s} = 172\ GeV)$ as given by eq. (6) (dashed) and the mean value of the radius distributed according to eq. (7) (full line), for $M_{\tilde{\chi}} = 50$ GeV/c^2 and $\Delta M = 200$ MeV/c^2. Moreover, not only the mean value changes because of the ISR: also the shape of the distribution of the decay radii does not follow a simple exponential law any longer. Figure 6b shows the ratio between the second moment of the ISR corrected distribution and that of an exponential with the same mean value. Thus, the best estimate of the experimental efficiency for detecting charginos of mass $M_{\tilde{\chi}}$ and degeneracy ΔM, in a given scenario, comes from the application of eq. (9).

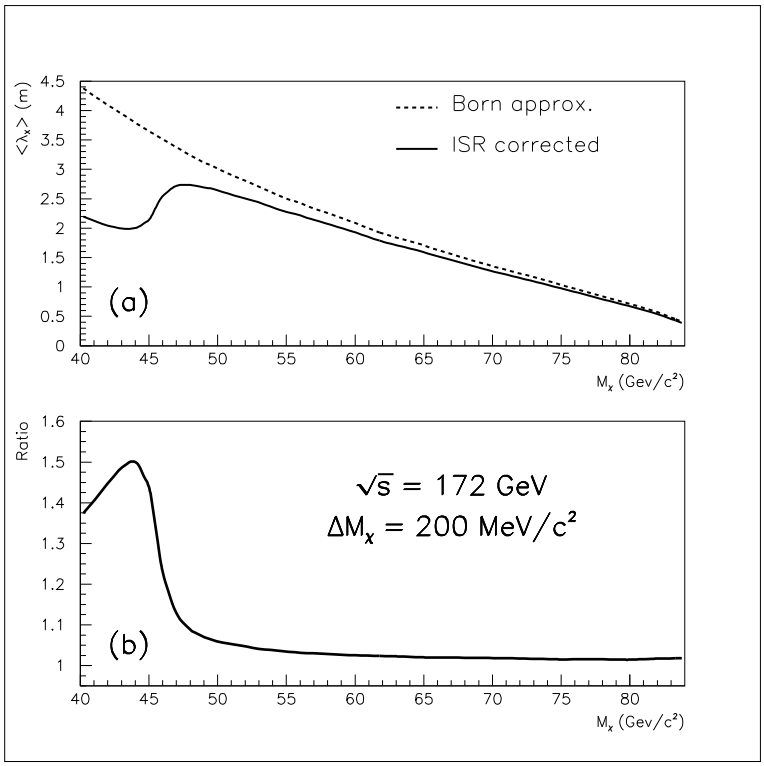

Figure 6: *(a) Mean decay lengths as a function of $M_{\tilde{\chi}}$ at a centre-of-mass energy of* 172 *GeV, for a degeneracy of* 200 *MeV/c^2 and for a heavy sneutrino. The approximation without ISR is shown by the dashed line and the effect of the ISR is shown by the full line. (b) Ratio between the second moment of the ISR-corrected distribution and the second moment of an exponential distribution for $\lambda_{\tilde{\chi}}$, with the same mean value, as a function of the mass of the chargino.*

4.4 Results

The search for heavy stable particles have been performed with all data collected at $\sqrt{s} = 130/136$, 161 and 172 GeV. No candidates remain in the data, whilst with the cuts used in [8], 2.5 ± 1.0 background events could be expected, mainly due to the coincidence of spurious hits in the two RICH radiators.

In the search for kinks, only data taken in 1996 at centre-of-mass energies of 161 and 172 GeV have been analyzed, and no candidates remain after the cuts.

These results, combined together, and the efficiencies given in the previous paragraphs yield the 95% confidence level (CL) exclusion regions in the plane $(M_{\tilde{\chi}}, \Delta M)$ shown in figure 7. Three cases (see section 3) are considered:

- low $|\mu|$, large $M_{1,2}$, any mass for the sfermions, any $\tan\beta$ and any R_f (higgsino-like);
- high $|\mu|$, low M_2, $m_{\tilde{\nu}} > 500$ GeV/c^2 (gaugino-like);
- high $|\mu|$, low M_2, light $m_{\tilde{\nu}}$ (gaugino-like).

The last two cases have been computed for $\tan\beta = 10$ and $R_f = 2$, although changes in these parameters result in minor variations of the exclusion limits. The limits obtained in the third case are much less significant than the other two. This is due to the fact that a light sneutrino increases the chargino decay width through virtual $\tilde{\nu}$ exchange. This is clearly seen by comparing the limit obtained for $M_{\tilde{\nu}} > M_{\tilde{\chi}} + 2$ GeV/c^2 with that for $M_{\tilde{\nu}} > M_{\tilde{\chi}} + 1$ GeV/c^2. Of course, whenever $M_{\tilde{\nu}} \leq M_{\tilde{\chi}}$ the exchanged sneutrino becomes real and the lifetime drops.

The efficiencies in [8] have been transformed in order to obtain the efficiency per track instead of the efficiency per event, so that they can be inserted into eq. (9). The efficiencies found in the search for kinks could be slightly overestimated for ΔM smaller than those used in the full simulation, because in that case the mean momentum, and so the detectability, is lower. In any case, this does not improve artificially the limits, because this region is already fully covered by the search for stable particles. The opposite happens at larger ΔM, where these efficiencies can be slightly underestimated: in that case, the limits reported in figure 7 are conservative. The same holds for the trigger efficiency. To be conservative, the smallest of the trigger efficiencies reported in table 1 is used in the analysis. An overestimate of the selection efficiency could take place for ΔM above 300 MeV/c^2, due to the opening of the hadronic channel, which has been switched off in the calculation of the lifetime in order to have a better agreement between the lifetime computed with the routines of SUSYGEN 2 and that computed with [10]. However, the conservative approximations used for the selection and trigger efficiencies are always compensating the loss of efficiency due to the reduced decay length resulting from the opening of the new channel.

In conclusion, in the whole space of the parameters spanned by the present search, the limits obtained are reliable, if not conservative.

5 Search for degenerate charginos with the tag of the photon ISR

For the search with an ISR photon tag, chargino production was simulated with $\Delta M =$ 0.5, 1 and 3 GeV/c^2. The criteria used to select events were defined on the basis of the simulated signal and background events. Charged particles were required to have a momentum above 100 MeV/c, known with an error below 100%, impact parameters below 4 cm in $r\phi$ and below 10 cm in z and a track length of at least 30 cm. To reduce the incidence of beam-gas events, a primary vertex compatible with the beam spot had to be reconstructed by using at least two of the charged particles.

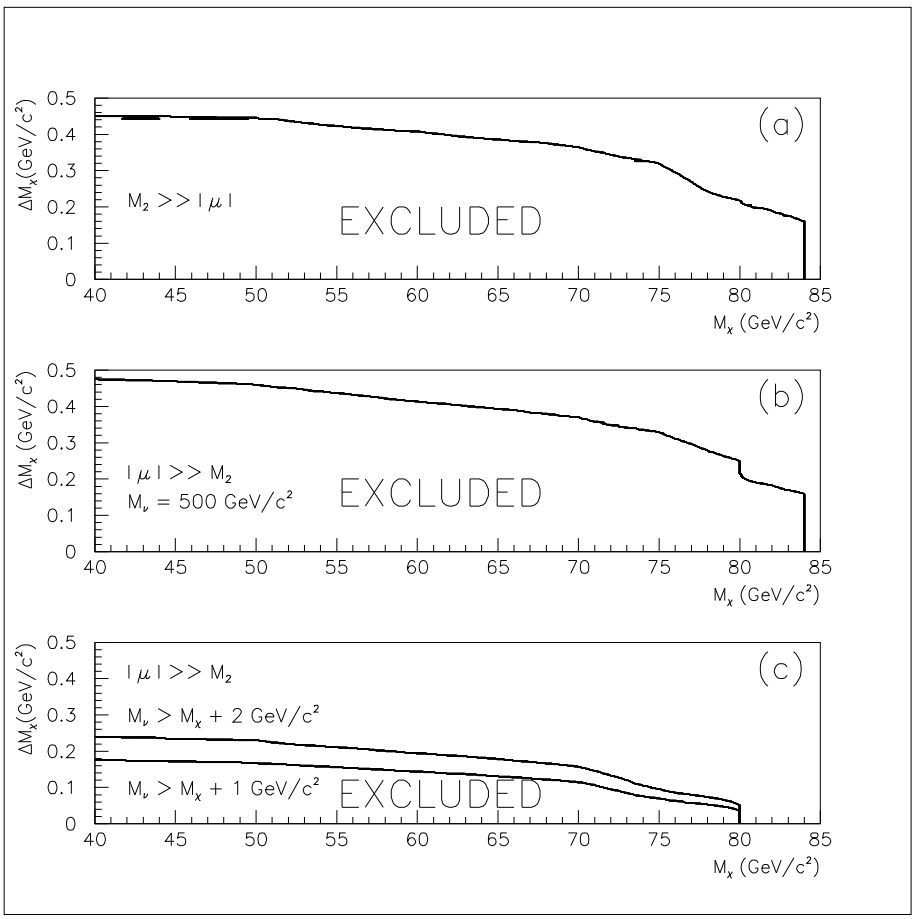

Figure 7: *Regions in the plane $(M_{\tilde{\chi}}, \Delta M)$ excluded at the 95% CL by the search for charginos with a visible decay length. (a) Higgsino-like scenario. (b)(c) Gaugino-like scenario, with the sneutrino mass set to 500 GeV/c^2 (b) or left free to vary above $M_{\tilde{\chi}} + 2$ GeV/c^2 and $M_{\tilde{\chi}} + 1$ GeV/c^2 (c).*

Neutrals had to have an energy of at least 500 MeV. Both calorimetric deposits and clear photon conversions in the material in front of the HPC were considered. To reduce the amount of noise in the calorimeters faking a neutral particle in the event, the following criteria have been used. In the HPC at least three of the nine layers must be hit; the first layer hit by the shower must be before the 6^{th} HPC layer; not more than 90% of the total energy of the shower can be deposited in a single layer; the θ angle reconstructed in the calorimeter must point to the main event vertex within 15^o. In the FEMC the shower must hit at least two towers. In the STIC an energy of more than 2 GeV must be associated to the shower and at least two towers must be hit.

All neutral showers inside a cone with half opening angle of 5^o are recombined together. If, after the recombination, the resulting neutral gets a fraction of hadronic energy above 10% of its total energy it will not be considered as an isolated ISR photon candidate.

All particles not having associated hits in any of the tracking devices of DELPHI have been considered as neutrals. Given the lower reconstruction and association efficiency of tracks in the two endcaps with respect to the barrel, tag electrons from $\gamma\gamma$ events can be seen as calorimetric deposits without the corresponding track elements: if that electron is isolated, it can fake an ISR photon, and special care must be paid to discard those events.

In the following, 'photon candidate' will mean a particle without track elements attached to it, not necessarily a 'real photon'.

5.1 Event selection

All the selection cuts are applied on a preselected sample containing events with at least two charged tracks. There should be an isolated photon candidate of at least 4 GeV, having a transverse energy above 2 GeV and a mass recoiling against it (M_{opp}) of at least 88 GeV/c^2. The isolation angle is at least 15^o from any other charged or neutral particle in the event. The visible energy of all particles excluding the photon should represent no more than 10% of the available centre-of-mass energy. Less than 99% of the whole visible energy must be in a single hemisphere inside a cone of half opening angle 60^o around the beam axis. The mass recoiling against the photon is

$$M_{opp}^2 = E_{cms}^2 - 2E_{cms}E_\gamma \tag{10}$$

and a lower limit on M_{opp} translates into an upper limit on the photon energy at each E_{cms}.

The selection criteria consist in some tightening of the preselection cuts in order to optimize the signal efficiency and the background rejection.

- The main cut against the $\gamma\gamma$ background is the one on the transverse photon energy, E_T^γ. The cut has been defined by inserting in equation (1) the minimum angle visible in the STIC, which is approximately 1.95^o; this automatically defines a different cut on E_T^γ at the different centre-of-mass energies.

- M_{opp} must be above 96 GeV/c^2. This cut is intended to reduce the rate of radiative Z^0 returns in the final sample.

- The photon is required to be isolated by at least 30^o with respect to any other charged or neutral particle in the event.

- The visible energy of the event, excluding the photon, must be below 5% of E_{cms}.

- The fraction of visible energy inside a double cone of 30^o (E_{30}/E_{vis}) or a single hemisphere cone of 60^o (E_{frw}/E_{vis}) both centred on the beam axis must be below, respectively, 60% and 80%. If the photon is inside the cone, its energy is subtracted both from the numerator and from the denominator which define the fractions.

- If there are more than two particles besides the photon in the event, their aplanarity must be above 0.005. The aplanarity is defined as the lowest normalized eigenvalue of the tensor of inertia.

- If the ISR photon candidate is in the STIC region, it must not be correlated with a signal in the corresponding Veto Counters [17].

Figures 8 and 9 show the distributions of the variables used in the selection for the preselected samples at 161 and 172 GeV respectively. The data are compared with the sum of all SM expectations. The agreement is quite reasonable in almost all distributions. The discrepancies that appear in some bins are due either to the limitations of the generators

used to simulate the background or to strong preselection cuts already present at the generation in the simulated samples. As discussed in section 2 the comparison of different generators of $\gamma\gamma$ events allows for a qualitative explanation of most of the problems. One should notice that all the discrepancies disappear after applying all cuts.

The corresponding distributions for charginos with $M_{\tilde{\chi}} = 50$ GeV/c^2 and $\Delta M = 1$ GeV/c^2 are shown in figures 8 and 9. In the plot of the visible energy are reported all the three degeneracies studied in detail, since the energy of the visible decay products depends on ΔM.

For the background estimates at $\sqrt{s} = 130{,}136$ GeV, the problems with the MC samples are still larger, since many of them have been generated with cuts stronger than those used afterwards during the analysis. A posteriori, since no candidates have been found at those energies, there is no need to have a precise evaluation of the background content to set the limits.

All these cuts have been defined by comparing signal and background MC's at 161 GeV and they rescale with the centre-of-mass energy.

5.2 Results

The results of the cuts on data and background MC at all the centre-of-mass energies are shown in table 2. No candidates remain at 130, 136 and 161 GeV while at 172 GeV one event survives all cuts. The expected background at the last two energies is respectively 0.82 ± 0.47 and 1.25 ± 0.58 events, while at 130 and 136 GeV no event remains in any of the background samples tested.

$\sqrt{s}$ (GeV)	$\mathcal{L}$ (pb^{-1})	Data	Background
130	2.86	0	$\simeq 0$
136	2.93	0	$\simeq 0$
161	9.70	0	0.82 ± 0.47
172	9.85	1	1.25 ± 0.58

Table 2: *Results of the selection on the data and on the expected SM background. The integrated luminosity is the one used for the analysis.*

The selection efficiency for degenerate charginos at all centre-of-mass energies is reported in table 3. The very low signal efficiency results from the requirement of a hard ISR photon: when the chargino mass increases, the ISR photon becomes softer, and so the overall event selection efficiency gets low. The efficiency have been checked to be the same independently on the specific final state of the chargino decay. This is easily understood, because all the decay modes of the degenerate charginos produce a charged (e, μ or π) and a neutral particle (ν_e, ν_μ or π^0), in addition to the neutralino, and the selection criteria rely mainly on the properties of the two charged tracks (besides the ISR photon).

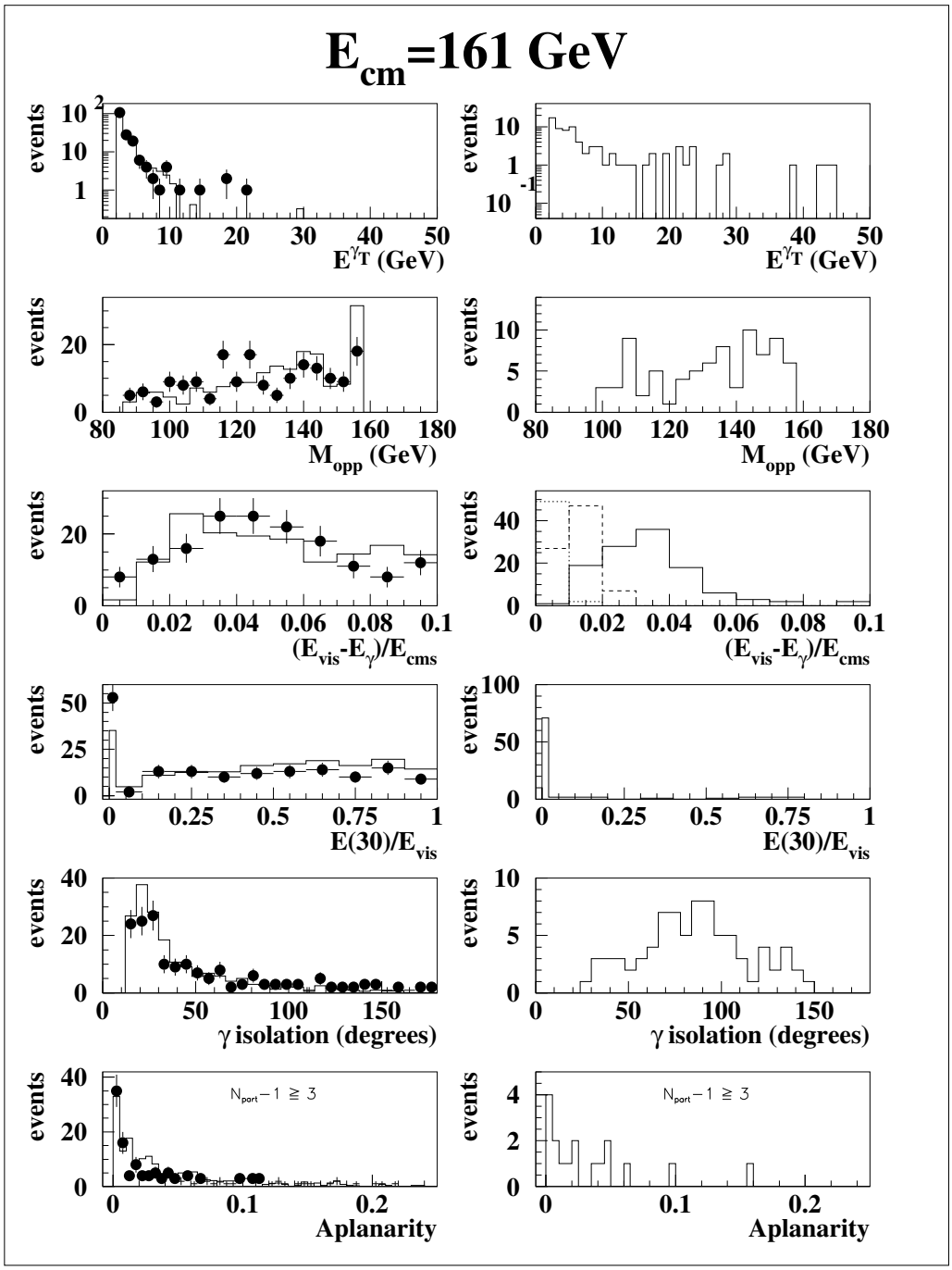

Figure 8: *Some of the variables used in the selection at 161 GeV. In the left plots the data (dots) are compared with the SM expectations. On the right, as an example, the corresponding distributions (with arbitrary normalization) are shown for the signal of mass 50 GeV/c^2 and $\Delta M = 1$ GeV/c^2. In the plot of the visible energy all the three degeneracies are shown for $M_\chi = 50$ GeV/c^2: dotted, $\Delta M = 0.5$ GeV/c^2; dashed, $\Delta M = 1$ GeV/c^2; full line, $\Delta M = 3$ GeV/c^2. In the plot of the aplanarity enter only events with more than three visible particles.*

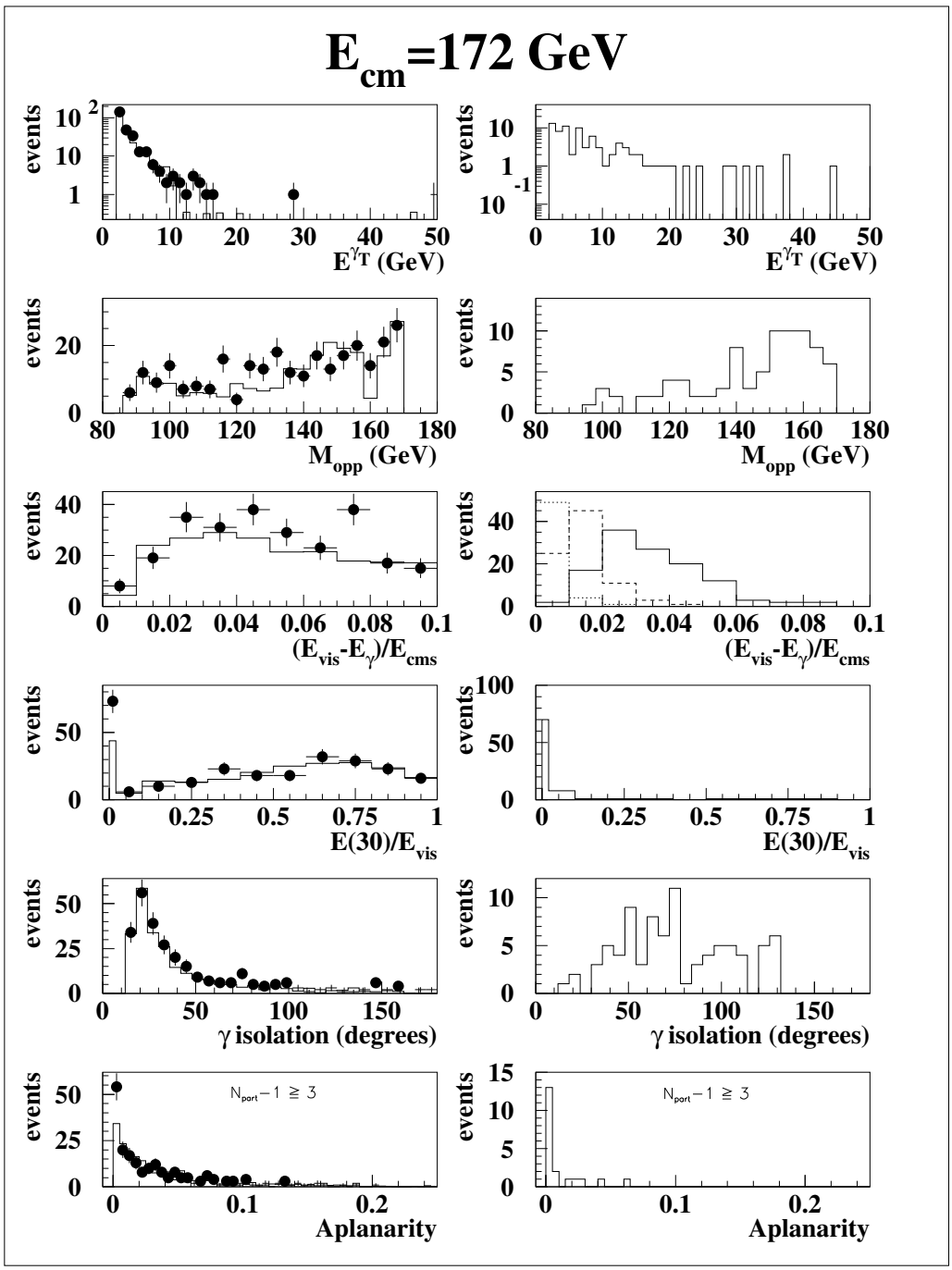

Figure 9: *Same as figure 8, but data and simulation refer to the samples at 172 GeV.*

	$M_\chi = 45$ (GeV/c^2)	$M_\chi = 50$ (GeV/c^2)	$M_\chi = 60$ (GeV/c^2)	$M_\chi = 70$ (GeV/c^2)
$E_{cms} = 130$ GeV				
$\Delta M = 0.5$	$(1.1 \pm 0.2)\%$	$(0.8 \pm 0.2)\%$	$(0.2 \pm 0.1)\%$	-
$\Delta M = 1.0$	$(1.4 \pm 0.3)\%$	$(0.9 \pm 0.2)\%$	$(0.2 \pm 0.1)\%$	-
$\Delta M = 3.0$ (GeV/c^2)	$(1.3 \pm 0.3)\%$	$(1.0 \pm 0.2)\%$	$(0.2 \pm 0.1)\%$	-
$E_{cms} = 136$ GeV				
$\Delta M = 0.5$	$(1.0 \pm 0.2)\%$	$(1.1 \pm 0.2)\%$	$(0.3 \pm 0.1)\%$	-
$\Delta M = 1.0$	$(2.0 \pm 0.3)\%$	$(1.1 \pm 0.2)\%$	$(0.2 \pm 0.1)\%$	-
$\Delta M = 3.0$ (GeV/c^2)	$(1.5 \pm 0.3)\%$	$(1.3 \pm 0.3)\%$	$(0.5 \pm 0.2)\%$	-
$E_{cms} = 161$ GeV				
$\Delta M = 0.5$	$(1.5 \pm 0.3)\%$	$(1.1 \pm 0.2)\%$	$(1.0 \pm 0.2)\%$	$(0.3 \pm 0.1)\%$
$\Delta M = 1.0$	$(2.7 \pm 0.4)\%$	$(2.2 \pm 0.3)\%$	$(1.1 \pm 0.2)\%$	$(0.6 \pm 0.2)\%$
$\Delta M = 3.0$ (GeV/c^2)	$(1.9 \pm 0.3)\%$	$(2.0 \pm 0.3)\%$	$(1.4 \pm 0.3)\%$	$(0.7 \pm 0.2)\%$
$E_{cms} = 172$ GeV				
$\Delta M = 0.5$	$(1.2 \pm 0.2)\%$	$(1.3 \pm 0.2)\%$	$(1.0 \pm 0.2)\%$	$(0.3 \pm 0.1)\%$
$\Delta M = 1.0$	$(1.6 \pm 0.3)\%$	$(1.9 \pm 0.3)\%$	$(1.3 \pm 0.3)\%$	$(0.8 \pm 0.2)\%$
$\Delta M = 3.0$ (GeV/c^2)	$(1.6 \pm 0.3)\%$	$(1.8 \pm 0.3)\%$	$(1.3 \pm 0.3)\%$	$(0.7 \pm 0.2)\%$

Table 3: *Selection efficiency for the chargino signal, computed at the different centre-of-mass energies as function of the chargino mass and mass difference with respect to the LSP.*

The trigger efficiency in DELPHI is practically 100% for most of the accessible final states. However, in the present search one looks for a few particles of very low momentum, accompanied by an energetic photon. Below transverse momenta of the order of 1-2 GeV/c the single track trigger efficiency starts to decrease [18]. For that reason a dedicated and detailed study of the trigger performances at low visible transverse energy has been carried out. The trigger efficiencies for events having a visible transverse energy, similar to the one of the system accompanying the ISR photon in the signal samples which pass the selection cuts, have been computed from the data. The events triggered by the STIC luminometer are to compute the low momentum trigger efficiency, because the soft particles are not triggered by the calorimeter. The overall trigger efficiency for the signal is then estimated as the logical OR of the known single photon trigger efficiency [19] and the low momentum trigger efficiency. Such an estimate could be conservative, because the coincidence of the photon and some of the remaining tracks can generate a further independent trigger signal.

Moving from E_{cms} = 130, 136 GeV to E_{cms} = 161, 172 GeV, the $\gamma\gamma$ cross section increases as well as the noise from the LEP machine. These processes produced an higher rate of the low P^T triggers. To keep the acquisition dead time at a reasonable low level, these trigger components were progressively scaled down. Therefore the 'non-photonic' trigger efficiency for the signal in the last two sets of data is reduced. Also the STIC single γ trigger was downscaled during some of the 172 GeV runs, but the overall trigger efficiency is not affected so much, because of the E_γ^T cut. Table 4 reports the trigger efficiencies estimated at the different centre-of-mass energies as a function of M_χ and ΔM.

A graphical view of the candidate remaining at 172 GeV is shown in figure 10. It consists of a 7.9 GeV photon in the HPC and two very acollinear and acoplanar charged tracks. These tracks have calorimetric deposits inconsistent to be identified as electrons, whilst the absence of hits in the muon chambers suggests that they are not muons either. There is some activity in the STIC and a deposit of 33.6 GeV in the Very Small Angle Tagger (VSAT), not visible in the figure. The VSAT is not used in the selection. This event is therefore perfectly consistent with a $\gamma\gamma$ event with hadronic final states. The energy of the charged particles is equal to $0.027 \cdot E_{cms}$. This value is inconsistent with all signal events having a mass difference of 500 MeV/c^2, is consistent with the ΔM = 3 GeV/c^2 signal and only slightly consistent with the ΔM = 1 GeV/c^2 one. In the calculation of the exclusion limits it will be considered as a candidate only for the charginos with a mass difference of 1 and 3 GeV/c^2.

5.3 Combination with the previous searches for charginos at $\Delta M = 3$ GeV/c^2

Although it has been verified that the search for charginos reported in [4] is completely blind already for ΔM = 1 GeV/c^2, at a degeneracy of 3 GeV/c^2 it shows still an efficiency which is comparable to the one obtained by the search for degenerate charginos which uses the ISR photon tag. Both signal and background events, selected by the two analyses, are typically different, since they look at the two opposite edges of the visible energy spectrum. Thus the combined efficiency is approximately the sum of the two efficiencies taken separately. The combined selection and trigger efficiencies are shown in table 5. They are computed on the same points at ΔM = 3 GeV/c^2 used for the search with the ISR photon.

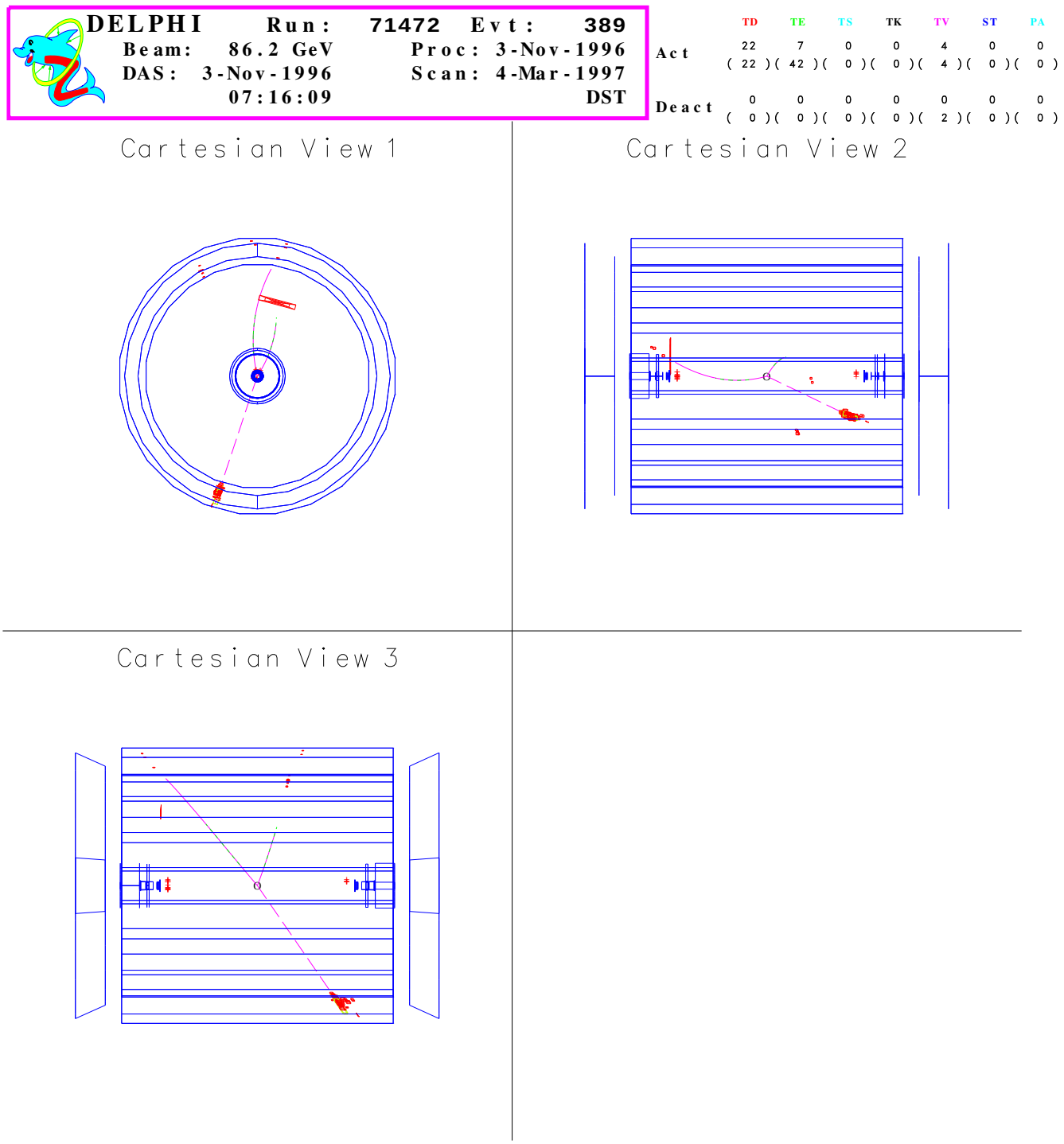

Figure 10: *The selected candidate in the search for charginos with degenerate mass with the LSP. Not visible in the picture, there are 33.6 GeV deposited in one sector of the VSAT. The photon in the HPC has an energy of 7.9 GeV. The sum of all other visible energies in the event (excluding the VSAT) is 4.7 GeV.*

	$M_\chi = 45$ (GeV/c^2)	$M_\chi = 50$ (GeV/c^2)	$M_\chi = 60$ (GeV/c^2)	$M_\chi = 70$ (GeV/c^2)
$E_{cms} = 130/136$ GeV				
$\Delta M = 0.5$	90.3%	88.9%	85.3%	-
$\Delta M = 1.0$	94.9%	95.0%	92.6%	-
$\Delta M = 3.0$ (GeV/c^2)	98.8%	99.2%	98.3%	-
$E_{cms} = 161$ GeV				
$\Delta M = 0.5$	88.5%	87.1%	85.4%	82.3%
$\Delta M = 1.0$	91.6%	90.7%	89.9%	86.0%
$\Delta M = 3.0$ (GeV/c^2)	97.3%	96.7%	95.5%	95.5%
$E_{cms} = 172$ GeV				
$\Delta M = 0.5$	87.0%	85.8%	83.5%	80.9%
$\Delta M = 1.0$	90.9%	89.0%	88.6%	84.2%
$\Delta M = 3.0$ (GeV/c^2)	95.8%	95.8%	93.8%	91.9%

Table 4: *Trigger efficiency for the chargino signal, computed at different centre-of-mass energies as function of the chargino mass and mass difference with respect to the LSP. The relative errors (not shown) are well below the selection efficiency ones and can be neglected when computing the upper limits on the mass of the chargino.*

As in the current search, also in the previously described selection [4] one candidate remains at the centre-of-mass energy of 172 GeV (the two candidates are different), compatible with the expected background contamination of 0.87 ± 0.08 events.

5.4 Exclusion limits in the search with the ISR tag

Since there is no evidence for a signal at any of the centre-of-mass energies studied, one can derive limits on the pair production of charginos mass-degenerate with the LSP.

Although the cross section is relatively high for all chargino masses (see figure 1), it is important to combine the data taken at all energies, because of the low signal efficiency.

The number of events expected from the four samples at 130, 136, 161 and 172 GeV is:

$$N_{exp} = \sum \sigma_i \mathcal{L}_i \, \varepsilon_i^{sel} \varepsilon_i^{trig} \tag{11}$$

	$M_\chi = 45$ (GeV/c^2)	$M_\chi = 50$ (GeV/c^2)	$M_\chi = 60$ (GeV/c^2)	$M_\chi = 70$ (GeV/c^2)
$\sqrt{s} = 130$	$(3.2 \pm .4)\%$	$(2.9 \pm .4)\%$	$(0.9 \pm .2)\%$	-
	0.993	0.994	0.991	-
$\sqrt{s} = 136$	$(3.6 \pm .4)\%$	$(3.3 \pm .4)\%$	$(1.5 \pm .3)\%$	-
	0.994	0.996	0.988	-
$\sqrt{s} = 161$	$(5.1 \pm .5)\%$	$(5.2 \pm .5)\%$	$(3.2 \pm .4)\%$	$(2.0 \pm .3)\%$
	0.988	0.985	0.977	0.975
$\sqrt{s} = 172$	$(5.3 \pm .5)\%$	$(5.4 \pm .5)\%$	$(3.9 \pm .5)\%$	$(2.8 \pm .4)\%$
	0.985	0.979	0.969	0.973

Table 5: *Selection (above) and trigger (below) efficiencies for charginos having a mass difference of 3 GeV/c^2 with the lightest neutralino (LSP). They are computed with the logical OR of the two selections whose efficiencies are detailed in table 3 and in [4].*

and its statistical distribution is determined by the (binomial) distribution of the four selection efficiencies. The error associated to the trigger efficiency becomes negligible in the product, given the large relative uncertainity on ε_i^{sel}.

The number of signal events compatible with the data and the computed background contamination follows a poissonian distribution in each channel. The distribution of the sum N_{up} of all the channels can be derived as suggested in [20].

The distribution of the difference $N_{exp} - N_{up}$ has been reconstructed with a MC in which the exact distributions of all the terms entering the expression are included [21].

Figure 11 shows the lower limit, at the 95% CL, of the difference $N_{exp} - N_{up}$, as a function of the mass of the chargino and for the degeneracies of 0.5, 1 and 3 GeV/c^2. Whenever the limit is above 0, the point $(M_{\tilde{\chi}}, \Delta M)$ can be excluded with the same confidence level. The upper part of the figure corresponds to the higgsino-like scenario, described in par. 3. The limit is computed in correspondence of the chargino masses of 45, 50, 60 and 70 GeV, for which a full simulation, with all detector effects, has been produced. The limit already obtained at LEP1 [5] cannot be improved at any of the three degeneracies studied.

In the gaugino-like scenario, shown in the bottom part of the figure 11, chargino masses below 53.4 GeV/c^2 can be excluded for any degeneracy between 0.5 and 3 GeV/c^2, provided $1 < \tan\beta < 50$ and $M_{\tilde{\nu}} > 500$ GeV/c^2. The interpolation between the points in which a full simulation is available has been obtained by using a fast simulation with SUSYGEN at the generator level as a guideline for the behaviour of the efficiency with respect to $M_{\tilde{\chi}}$. For the common limit, the most conservative between those computed in correspondence of $\Delta M = 0.5$, 1 and 3 GeV/c^2 has been kept. The details of the 95% CL limits obtained for the three degeneracies are shown in table 6

The same method allows to set a limit in the case in which the ISR analysis is combined

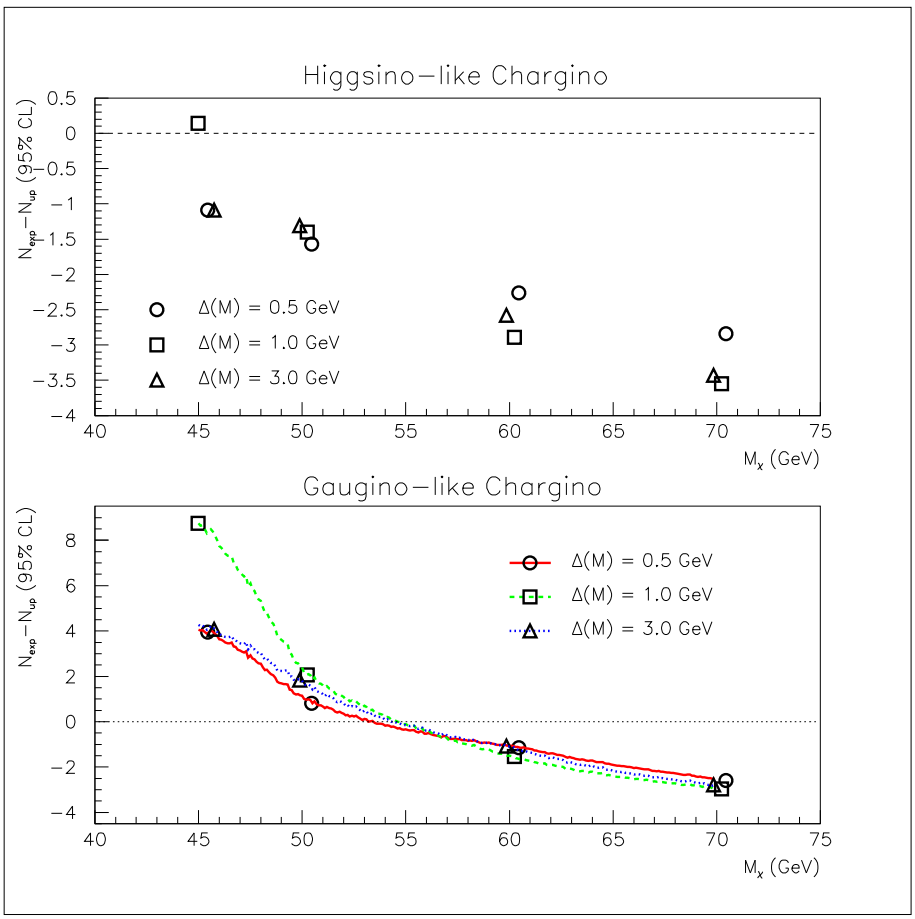

Figure 11: *Lower limit at the 95% CL of the difference between the number of chargino events expected and the ones allowed in the data (it depends on the candidates found and on the background computed), as a function of the chargino mass. Whenever this limit is above 0, the point can be excluded at 95% CL.*

with the previous analyses at $\Delta M = 3$ GeV/c^2 as described in 5.3. The 95% CL lower limits on $M_{\tilde{\chi}}$ are 56.8 GeV/c^2 for the higgsino-like chargino and 66.9 GeV/c^2 for the gaugino-like chargino, with the same range of variability of the SUSY parameters as reported above. These results allow to exclude a larger mass region with respect to what reported in [4].

6 Conclusions

A first attempt to look for sparticles mass-degenerate with the LSP has been made using the data collected by the DELPHI experiment during the runs of LEP above the Z^0 pole energy. Two different approaches are used to detect charginos with degenerate mass with respect to the lightest neutralino, supposed to be the LSP.

For extremely degenerate charginos ($\Delta M < 500$ MeV/c^2) it is exploited the information contained in their long lifetime (decay length). The search for heavy particles decaying outside the central subdetectors of DELPHI is done by looking at the specific ionization of the tracks in the TPC and at the light cone produced in the RICH detector. Chargino decays, roughly between 10 cm and 1 m, would be seen by searching for kinks

ΔM (GeV/c^2)	95% CL
0.5	53.4 GeV/c^2
1	54.5 GeV/c^2
3	54.4 GeV/c^2

Table 6: 95% *confidence level upper limits on the mass of the gaugino-like chargino at the three degeneracies tested.*

in the tracks reconstructed in the central tracking devices of DELPHI. Both searches end up with no candidates, when applied to the data collected at 130, 136, 161 and 172 GeV (the first analysis) and at 161 and 172 GeV (the second analysis). Given the experimental results, the 95% CL exclusion plots in the plane $(M_{\tilde{\chi}}, \Delta M)$ can be derived, as shown in figure 7.

When the lifetime is so short that the decay vertex can be hardly distinguished from the interaction one and ΔM is too small ($0.5 < \Delta M < 3$ GeV/c^2) to be selected by the usual criteria adopted in the search for charginos, the events can be partially recovered by looking for the typical topologies of the degenerate charginos accompanied by an high energy photon radiated from the initial state. The ISR tag reduces the otherwise overwhelming two photon background to acceptable rates, although it also strongly affects the signal efficiency. It is necessary to combine all the statistics collected so far at the different LEP2 centre-of-mass energies to get sensitivity of the signal. No evidence of it has been found in the data collected by DELPHI at the centre-of-mass energies of 130, 136, 161 and 172 GeV. The existence of charginos having a mass difference with the LSP between 0.5 and 3 GeV/c^2 can be excluded at the 95% confidence level for $M_{\tilde{\chi}_1^+} < 53.4$ GeV/c^2, provided the chargino is gaugino-like and the mass of the sneutrino is above 500 GeV/c^2.

Combining the previously reported [4] selection for charginos with the ISR tag described here, charginos with a mass degeneracy of 3 GeV/c^2 with the lightest neutralino can be excluded at the 95% CL up to masses of 56.8 GeV/c^2, if higgsino, or 66.9 GeV/c^2, if gaugino and $M_{\tilde{\nu}} > 500$ GeV/c^2.

Acknowledgements

We would like to thank M. Drees for providing the program to compute the chargino branching ratios at low ΔM; P. Kluit for the details of the search for 'stable' partyicles; S. Katsanevas for explaining the features of SUSYGEN; V. Canale and G. Valenti for their support in analizing the data of the DELPHI trigger; J. Guy for his help in producing the full simulation of our special MC samples; André Sopczak for several stimulating discussions.

References

[1] H. P. Nilles, Phys. Rep. **110** (1984) 1;
H.E. Haber and G.L. Kane , Phys. Rep. **117** (1985) 75.

[2] P.F. Smith, et al., Nucl. Phys. **B206** (1982) 333.

[3] P. Abreu et al. (DELPHI Coll.), Phys. Lett. **B382** (1996) 323;
P. Abreu et al. (DELPHI Coll.), Phys. Lett. **B387** (1996) 651.

[4] P. Abreu et al. (DELPHI Coll.), Search for chargino, neutralino and gravitino at LEP, *paper presented at the ICHEP 97 conference*

[5] Particle Data Group J.J.Hernandez et al., Phys. Rev. **D54** (1996).

[6] A. Brignole, L.E. Ibañez, C. Muñoz, Nucl. Phys. **B422** (1994) 125.

[7] C.H. Chen, M. Drees, J.F. Gunion, Phys. Rev. **D55** (1997) 330.

[8] P. Abreu et al. (DELPHI Coll.), Phys. Lett. **B396** (1997) 315.

[9] P. Abreu et al. (DELPHI Coll.), s-lepton Search in degenerate scenarios, *paper presented at the ICHEP 97 conference*

[10] C.H. Chen, M. Drees, J.F. Gunion, Phys. Rev. Lett. **76** (1996) 2002.

[11] P. Aarnio, et al., (DELPHI Coll.), Nucl. Inst. Meth. **A303** (1991) 233;
P. Abreu, et al, (DELPHI Coll.), Nucl. Inst. Meth. **A378** (1996) 57.

[12] T. Sjöstrand, Comp. Phys. Comm. **39** (1986) 347;
T. Sjöstrand, "PYTHIA 5.6 and JETSET 7.3", CERN-TH/6488/92.

[13] DELSIM users guide and reference manual, DELPHI 89-15 PROG 130 and 89-69 PROG 143.

[14] S. Katsanevas and S. Melanchroinos in "Physics at LEP2", CERN 96-01 (Vol.2) 328.

[15] F.A. Berends, P.H. Daverveldt, R. Kleiss, Nucl. Phys. **B253** (1985) 421;
Comp. Phys. Comm. **40** (1986) 271, 285 and 309.

[16] S. Nova, A. Olshevskyi, T. Todorov, DELPHI 90-35 PROG 152.

[17] A.C. Benvenuti, et al., IEEE Trans. Nucl. Sci. **40** (1993) 537.

[18] V. Bocci, et al., Nucl. Inst. Meth. **A362** (1995) 361.

[19] P. Abreu, et al. (DELPHI Coll.) Zeit. Phys. **C74** (1997) 577;
W. Adam, et al. (DELPHI Coll.), Phys. Lett. **B380** (1996) 471.

[20] V.F. Obraztsov, Nucl. Inst. Meth. **A316** (1992) 388;
O. Helene, Nucl. Inst. Meth. **212** (1983) 319.

[21] A. Perrotta, DELPHI 97-36 PHYS 689.